INTERNATIONAL JOURNAL FOR NUMERICAL METHODS IN FLUIDS
Int. J. Numer. Meth. Fluids 2005; **47**:1101–1106
Published online 31 January 2005 in Wiley InterScience (www.interscience.wiley.com). DOI: 10.1002/fld.864

Incompressible separated flows simulations with the smoothed particle hydrodynamics gridless method

R. Issa[1,*,†], E. S. Lee[1], D. Violeau[2] and D. R. Laurence[1]

[1]*UMIST/MAME Department, Thermo-Fluids Division, Sackville St., G. Begg bldg, Manchester M60 1QD, U.K.*
[2]*EDF/Laboratoire Nationale d'Hydraulique et Environnement 6, quai Watier, 78 400 Chatou, France*

SUMMARY

The gridless Lagrangian method smoothed particle hydrodynamics (SPH) is preferentially used in CFD to simulate complex flows with one or several convoluted free surfaces. Indeed, this type of flow would require distorted meshes with Lagrangian finite difference methods or very fine meshes with VOF. As the literature is quite scarce concerning SPH validations for academic problems, we present in this paper some results relative to laminar recirculating flows. The ability of SPH to reproduce recirculation zone is revealed through a 2D hill and a backward-facing step geometry: axial velocity profiles obtained with SPH are quite satisfactory and separation and reattachment points are well predicted in both cases. Moreover, some practical and robust wall modelling conditions are also introduced and the limitation of the nearly incompressible assumption, used in most standard SPH codes, is illustrated. Indeed, we reveal that it is necessary to consider a relatively high speed of sound in order to avoid numerical voids. Copyright © 2005 John Wiley & Sons, Ltd.

KEY WORDS: hill channel; backward-facing step; wall modelling; nearly incompressible assumption

1. INTRODUCTION

The smoothed particle hydrodynamics (SPH) numerical method is successfully applied in fluid mechanics to simulate delicate free surface flows (dam breaking, wave flumes, etc.) which would require complex meshes with classical Eulerian code. SPH is very efficient for rapid, convection dominated flows where turbulence or viscous effects are negligible. However, the validations are fairly qualitative and as noted by Morris [3], it is not so easy to thoroughly test the SPH method on equilibrium, academic flows, in particular with recirculation zones. For this purpose, this paper presents results relative to laminar separated flows in a 2D hill and a backward-facing step geometry. Moreover, practical boundary conditions are presented

*Correspondence to: R. Issa, EDF R&D, LNHE (P75) 6, quai Watier, 78 401 Chatou, France.
†E-mail: r.issa@postgrad.umist.ac.uk, reza.issa@edf.fr

Received 27 April 2004
Revised 3 September 2004
Accepted 14 September 2004

and the limitation of the nearly incompressible assumption, used in most standard SPH codes, is also illustrated.

2. THE SPH METHOD

2.1. Heart of the method

In SPH formalism, the fluid is discretized with a finite number of macroscopic fluid particles. Each particle a is characterized by a mass m_a, a density ρ_a, a pressure p_a, a velocity vector $\boldsymbol{u}_a$ and a position vector $\boldsymbol{r}_a$. At the heart of SPH is the interpolation formula (1) which evaluates the value of any flow property A at the position $\boldsymbol{r}$, in relation with all other fluid particles b

$$A(\boldsymbol{r}) = \sum_b \frac{m_b}{\rho_b} A_b w_h(\boldsymbol{r} - \boldsymbol{r}_b, h) + O(h^2) \tag{1}$$

Here w_h is an interpolating function which plays a central part in SPH: it depends on the distance between two particles and a parameter h called the smoothing length, here proportional to the initial particle spacing. In order to reduce the number of particles b involved in Equation (1) (and thus to reduce the calculation time), it is convenient to consider kernels characterized by a compact support of radius h_t, proportional to the smoothing length h. Consequently, only particles b located in the disc (or sphere, in 3D) of radius h_t and centred on a will contribute to the evaluation of the function A relative to the particle a. General expressions of kernels are given by Morris [3] and Monaghan [1]. In most SPH codes, spline kernels are used and we consider here the fourth-order spline kernel [6].

2.2. Fluid mechanics equations in SPH formalism

- An SPH form of the Lagrangian continuity equation can be written as

$$\frac{\mathrm{d}\rho_a}{\mathrm{d}t} = \sum_b m_b \boldsymbol{u}_{ab} \dot{w}_h(r_{ab}) \boldsymbol{\epsilon}_{ab} \tag{2}$$

  where $\boldsymbol{u}_{ab} = \boldsymbol{u}_a - \boldsymbol{u}_b$ and $\boldsymbol{\epsilon}_{ab} = \boldsymbol{r}_a - \boldsymbol{r}_b / r_{ab}$. $\dot{w}_h$ corresponds to the spatial partial derivative of the kernel and $\mathrm{d}/\mathrm{d}t$ to a Lagrangian derivative obtained by following the motion of a particle.
- In a Lagrangian form, the equation of motion is

$$\frac{\mathrm{d}\boldsymbol{u}}{\mathrm{d}t} = -\frac{1}{\rho} \boldsymbol{\nabla} p + v \triangle \boldsymbol{u} + \boldsymbol{F}^{\mathrm{e}} \tag{3}$$

  where v denotes the kinematic viscosity of the fluid, p the pressure, ρ the density and $\boldsymbol{F}^{\mathrm{e}}$ external forces such as gravity or Lorentz force in magnetohydrodynamics.

  If the continuity equation (2) is used, Bonet [4] proved that the pressure gradient term must be discretized according to

$$\boldsymbol{\nabla} p_a = \sum_b \frac{m_b}{\rho_b} (p_b + p_a) \dot{w}_h(r_{ab}) \boldsymbol{\epsilon}_{ab} \tag{4}$$

In SPH theory, viscous effects are commonly modelled by an artificial pressure [1, 9] according to

$$\nu \triangle \boldsymbol{u}_a = \sum_b m_b \frac{16\nu}{\rho_a + \rho_b} \frac{\boldsymbol{u}_{ab}.\boldsymbol{r}_{ab}}{r_{ab}^2 + \eta^2} \dot{w}_h(r_{ab}) \boldsymbol{\epsilon}_{ab} \tag{5}$$

with $\eta^2 = 0.01h^2$ introduced to avoid a zero denominator and $\boldsymbol{r}_{ab} = \boldsymbol{r}_a - \boldsymbol{r}_b$.

- The pressure of each particle is determined with the following stiff state equation [10]:

$$p(\rho) = \frac{\rho_0 c_0^2}{\gamma} \left[\left(\frac{\rho}{\rho_0} \right)^{\gamma} - 1 \right] \tag{6}$$

where ρ_0 represents a reference density, c_0 a numerical speed of sound and γ a constant coefficient equal to 7. In order to simulate a nearly incompressible flow, c_0 must be at least ten times superior than the maximal velocity of the flow. This nearly-incompressible assumption thus induces a Mach number M less than 0.1. Consequently, the relative variation of density, which scales as M^2 [3], is less than 1%.

3. LAMINAR 2D HILL FLOW

3.1. Geometry of the system

We consider the 2D hill defined in ERCOFTAC workshop [11] and represented in Figure 1 (left). Periodic conditions are applied with respect to x-direction, in order to represent an infinite hill channel.

3.2. Fluid and wall discretization

The fluid is discretized with 19 548 particles spaced by $\delta r = 1\,\text{mm}$. These particles are initially placed on a regular Cartesian lattice and contrary to classical Eulerian codes, there is no need to refine the mesh near the wall in the considered case. The wall is modelled with solid particles called wall particles. Moreover, in order to ensure the impermeability of the wall, three layers of mirror particles are added under the wall: the density of wall and mirror particles evolves thanks to the contribution of fluid particles through the continuity equation (2). Indeed, if the fluid particle a is linked to the solid or mirror particle b, the b-contribution to the evolution of a-density is equal to

$$m_b \boldsymbol{u}_{ab} \dot{w}_h(r_{ab}) \tag{7}$$

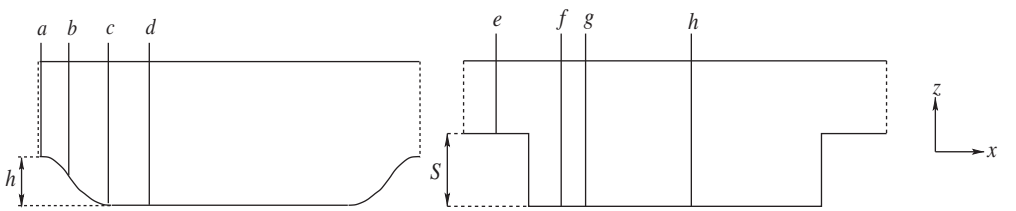

Figure 1. Geometry of the 2D hill channel (left) and the backward-facing step (right), with four profiles in each case.

As the particle b is also linked to the fluid particle a, the contribution of the particle a to the evolution of b-density is also given by Equation (7), since the continuity equation (2) is symmetric with respect to a and b subscripts. The pressures of wall and mirror particles are then computed with the state equation and these particles are involved in the pressure gradient relative to fluid particles. These new wall conditions also enable a perfect impermeability of the wall in rapid dynamic phenomena such as dam breaking. Contrary to the repulsive forces commonly used in SPH to represent wall [1], the present formulation does not introduce any *ad hoc* coefficient. Moreover, in contrast to traditional mirror particles used in most SPH codes, the method proposed here considers fixed particles and can be easily programmed.

3.3. Simulation conditions

A laminar flow of water in the 2D hill channel is investigated. The Reynolds number, based on the mean bulk velocity, the hill height h and the kinematic viscosity, is equal to 50. In order to reach this value, a propelling horizontal force per mass F is applied to each particle and is updated at each time step to impose the correct mass flow rate [6].

3.4. Results relative to the 2D hill flow

As there are no theoretical solutions for this problem, the results obtained with SPH are compared to those obtained by an unstructured Eulerian code based on finite volume method [11]. For this type of academic laminar flows, the solution given by the Eulerian code is considered as a reference one. We compare here axial velocity relative to four of the ten profiles defined in ERCOFTAC workshop [11] and represented in Figure 1. Figures 2(a)–(d) reveal that axial velocity profiles obtained with SPH are quite close to those obtained with the Eulerian code.

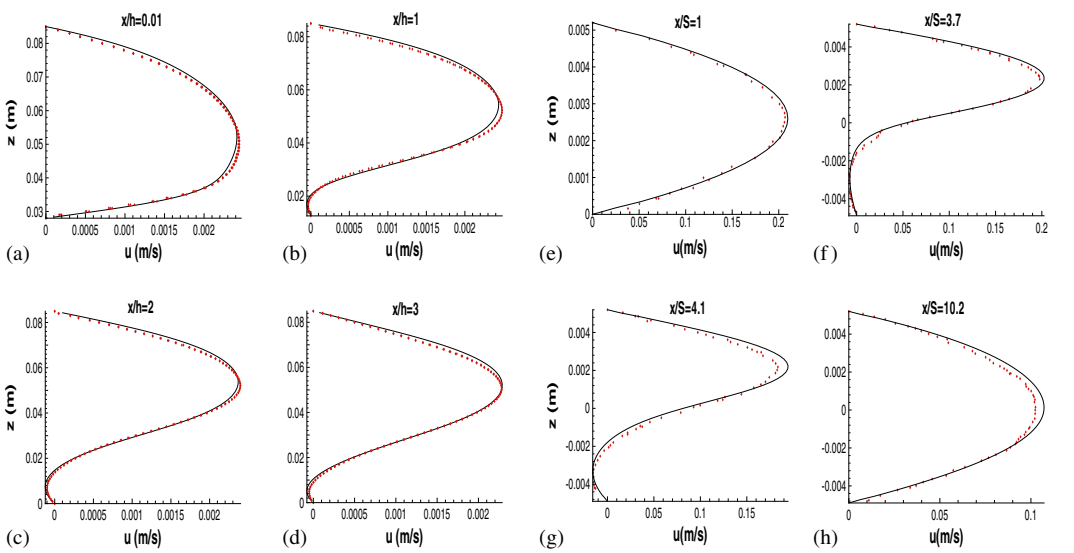

Figure 2. Axial velocity profiles obtained with an Eulerian code (—) and SPH (•) for the 2D hill (a)–(d) and the backward facing step geometry (e)–(h). h is the hill height and S the step height.

The profiles located in the vicinity of the hill reveal the presence of the recirculation zone. It has also been determined that SPH has an error of 0.7% (compared to the Eulerian code) for the separation point prediction and an error of 4.3% for the reattachment point prediction. In this last case, the error is more significant, due to the Lagrangian characteristic of SPH: indeed, the determination of this length is quite delicate.

4. LAMINAR BACKWARD-FACING STEP

A backward-facing step is considered here to anchor the separation point. The separation occurs here at the step position.

4.1. System modelling

The geometry of the backward-facing step is based on the one used by Armaly [12] and represented in Figure 1 (right). However, for reasons of convenience, we add another step at the end of the channel in order to apply periodic conditions with respect to the x-direction. The fluid is discretized with nearly 46 000 particles and the initial inter-particle distance δr is decided from that 30 particles are placed along the step height. The wall modelling is identical to the previous case. We consider a flow of air, characterized by a Reynold number of 100 based on the mean bulk velocity, a length equal to twice the inlet height and the kinematic viscosity of the air [12].

4.2. Results

At first, the speed of sound is ten times superior to the maximal velocity of the flow, according to the nearly-incompressible assumption. As shown in Figure 3 (left), a large void appears next to the step. This means that the pressure gradient term is not high enough in this zone. Once a void appears, the pressure gradient cannot increase any more as there are no particles in the void to account for this depression. A way of increasing the range of admissible pressure values is to alter the compressibility. According to Equation (6), the pressure of particle (and consequently the pressure gradient term) is increased with a higher speed of sound.

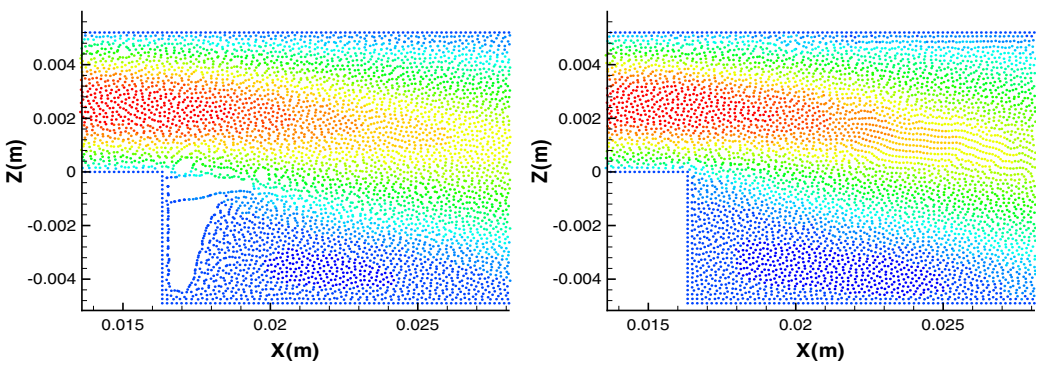

Figure 3. Void due to the nearly incompressible assumption (left) and correction with a higher speed of sound (right) in the case of the backward-facing step.

By increasing the numerical speed of sound by a factor 4 (which means that the speed of sound is now forty times higher than the maximal velocity of the flow), the void no longer appears (see Figure 3 (right)) and the recirculation zone is well established. However, increasing the speed of sound also induces smaller time steps due to the CFL condition [6]. Four velocity profiles, represented in Figure 2, are compared with the results of an Eulerian code based on finite volume. There is a good agreement between the velocity profiles at each position (see Figure 2(e)–(h)). Moreover, the reattachment point positions relative to SPH, the Eulerian code and the experiments correspond to $x/S = 6$, 6.7 and 6.3, respectively.

5. CONCLUSION

The ability of SPH to simulate a separated flow has been investigated through a 2D hill flow. In this case, the nearly-incompressible assumption gives satisfactory velocity profiles and the separation and reattachment points are well predicted. However, by considering laminar flow over a 2D backward-facing step geometry, it has been revealed that SPH with artificial compressibility is prone to creating bubbles of void in recirculation regions. Although the compressibility effect for a Mach number of 0.1 is generally considered acceptable as a nearly-incompressible flow approximation, SPH behaves as a rarefied gas in regions of low pressure. Only with a corrected Mach number of 0.025 was it possible to simulate a separated flow in a backward-facing step geometry. The parameters which describe the recirculation zone are then in good agreement with those obtained with a classical Eulerian code. Moreover, we introduced practical wall conditions with mirror particles to ensure a total impermeability of the wall. The following part of this work will be to develop a fully incompressible SPH method and to adapt large eddy simulation concept to SPH to treat turbulent effects.

REFERENCES

1. Monaghan JJ. Smoothed particle hydrodynamics. *Annual Review of Astronomy and Astrophysics* 1992; **30**: 543–574.
2. Swegle JW, Hicks DL, Attaway SW. Smoothed particle hydrodynamics stability analysis. *Journal of Computational Physics* 1995; **116**:123–134.
3. Morris JP, Fox PJ, Zhu Y. Modelling low Reynolds number incompressible flows using SPH. *Journal of Computational Physics* 1997; **136**:214–226.
4. Bonnet J, Lok T-SL. Variational and momentum preservation aspects of smooth particle hydrodynamics. *Computer Methods in Applied Mechanics and Engineering* 1999; **180**:97–115.
5. Ferziger JH, Peric M. *Computational Methods for Fluid Dynamics*. Springer: Berlin, 1996.
6. Issa R, Violeau D, Laurence DR. Smoothed particle hydrodynamics method for free surface flows. *IAHR Journal* 2003, submitted.
7. Gingold RA, Monaghan JJ. Kernel estimates as a basis for general particle methods in hydrodynamics. *Journal of Computational Physics* 1992; **46**:429–453.
8. Shao L, Sarkar S, Patano C. On the relationship between the mean flow and subgrid stresses in large eddy simulations of turbulent shear flows. *Physics of Fluids* 1999; **11**(5):1229–1248.
9. Shao S, Lo EYM. Incompressible SPH-method for simulating Newtonian and non-Newtonian flows with a free surface. *Advances in Water Resources* 2003; **26**:787–800.
10. Monaghan JJ. Simulating gravity currents with SPH III boundary forces, University of Monash. *Mathematics Reports and Preprints* 1995; **95**(5):1–8.
11. Alemida GP, Durao DFG, Heitor MV. Data available via www.ercoftac.org in 'classic database'. *Experimental and Thermal Fluid Sciences* 1993; **7**:87–101.
12. Armaly BF, Durst F, Pereira JCF, Schonung B. Experimental and theoretical investigation of a backward-facing step. *Journal of Fluid Mechanics* 1983; **127**:473–496.

